Phase Behavior of Blends of Styrene/Maleic Anhydride Copolymers

P. P. GAN and D. R. PAUL*

Department of Chemical Engineering and Center for Polymer Research, University of Texas at Austin, Austin, Texas 78712

SYNOPSIS

The phase behavior of blends of styrene/maleic anhydride copolymers (SMA) with styrene/methyl methacrylate copolymers (SMMA), styrene/acrylonitrile copolymers (SAN), tetramethyl bisphenol-A polycarbonate (TMPC), and poly(2,6-dimethyl-1,4-phenylene oxide) (PPO) have been determined. Tentative binary interaction energies were evaluated from mapping the copolymer composition miscibility boundaries using the Flory–Huggins theory combined with the binary interaction model. Data on phase-separation temperatures were too sparse for these systems to obtain refined estimates using the Sanchez–Lacombe theory. A negative interaction energy was obtained for the MA/AN pair; however, the MA unit showed strong repulsive interactions with all other monomer units examined here. © 1994 John Wiley & Sons, Inc.

INTRODUCTION

Miscible blends in which one component contains reactive functional groups are of interest as a route to controlling morphology and strengthening the interfacial zone, via reactive compatibilization, in multiphase polymer alloys.[1-16] Styrenic copolymers containing acid, anhydride, and epoxy units have been used for this purpose. In this article, the phase behavior of blends of styrene/maleic anhydride copolymers (SMA) with styrene/methyl methacrylate copolymers (SMMA), styrene/acrylonitrile copolymers (SAN), tetramethyl bisphenol-A polycarbonate (TMPC), and poly(2,6-dimethyl-1,4-phenylene oxide) (PPO) have been examined. Quantitative information about polymer–polymer interactions were evaluated where possible from the phase behavior of these blends using either the Flory–Huggins theory or the lattice fluid theory of Sanchez and Lacombe[17-19] combined with the binary interaction model. Expansion and refinement of the matrix of binary interaction energies[1-4,20-27] is needed for the rational design of such multicomponent blend systems.

* To whom correspondence should be addressed.

Journal of Applied Polymer Science, Vol. 54, 317–331 (1994)
 CCC 0021-8995/94/030317-15

THEORY

Certain aspects of the experimental phase behavior for polymer blends can be analyzed to obtain interaction energies using the elementary Flory–Huggins theory; however, some features commonly observed are thought to be better described by equation-of-state approaches like the Sanchez–Lacombe theory. For the former, the free energy of mixing per unit volume is given by

$$\Delta g_{\text{mix}} = RT\left[\frac{\phi_A \ln \phi_A}{\tilde{V}_A} + \frac{\phi_B \ln \phi_B}{\tilde{V}_B}\right] + B\phi_A\phi_B \quad (1)$$

where R is the universal gas constant; T, the absolute temperature; and ϕ_i and $\tilde{V}_i$, the volume fraction and molar volume of component i, respectively. The first term represents the combinatorial entropy, whereas the second term includes the enthalpic and excess entropic contributions expressed in a van Laar form. If the interaction energy in eq. (1) does not depend on composition, differentiation leads to the familiar spinodal equation

$$\frac{d^2\Delta g}{d\phi_1^2} = RT\left(\frac{1}{\phi_A\tilde{V}_A} + \frac{1}{\phi_B\tilde{V}_B}\right) - 2B_{\text{sc}} = 0 \quad (2)$$

where B_{sc} is the interaction parameter at the spinodal condition. When the interaction energy depends on composition, eq. (2) amounts to the definition of a new interaction energy. The subscript sc will be omitted in the following discussions. The condition for miscibility is

$$B < B_{crit} = \frac{RT}{2}(\tilde{V}_A^{-1/2} + \tilde{V}_B^{-1/2})^2 \quad (3)$$

The boundary between regions of miscibility and immiscibility is defined by $B = B_{crit}$.

For a binary blend of a random copolymer A composed of units 1 and 2 and a homopolymer composed of unit 3, the net interaction energy according to the binary interaction model is given by

$$B = B_{13}\phi_1' + B_{23}\phi_2' - B_{12}\phi_1'\phi_2' \quad (4)$$

where ϕ_i' is the volume fraction of i in the copolymer. For blends of copolymer A, composed of units 1 and 2, and copolymer B, composed of units 1 and 3, the net interaction energy is given by

$$B = B_{12}\phi_2'(\phi_2' - \phi_3'') + B_{13}\phi_3''(\phi_3'' - \phi_2') + B_{23}\phi_2'\phi_3'' \quad (5)$$

where the ϕ_i' and ϕ_i'' denote the volume fraction of unit i in copolymers A and B, respectively.

For blends of two copolymers that do not have a common monomer, e.g., copolymer A is composed of units 1 and 2 and copolymer B is composed of units 3 and 4, there are altogether six B_{ij} values. When the weight-average molecular weights or molar volumes of the components are fixed for this system, this theory predicts an elliptical, a parabolic, or a hyperbolic isothermal map of copolymer compositions dividing miscible from immiscible mixtures. Fitting the theory to an experimentally determined copolymer–copolymer isothermal miscibility map can give some information about the B_{ij} set; however, generally at least one B_{ij} value has to be obtained from another experiment in order to determine all the B_{ij} values. For copolymer–copolymer blends where there is a common monomer, as examined here, there are only three B_{ij} and, in principle, absolute values of all of these can be deduced from mapping the copolymer–copolymer composition miscibility boundaries.[28]

Equation-of-state theories are able to predict LCST behavior stemming from the compressible nature of materials, which is not taken into account in the simple Flory–Huggins theory. Thus, such theories are able to make more use of phase diagram information than can the simple isothermal mapping of the boundary between miscible and immiscible regions. The lattice-fluid theory of Sanchez–Lacombe can be employed to describe such effects. Detailed descriptions of this theory and its application to polymer blends are available elsewhere.[1,17–27] The lattice-fluid equation of state has the following simple closed form:

$$\tilde{\rho}^2 + \tilde{P} + \tilde{T}\left[\ln(1-\tilde{\rho}) + \left(1 - \frac{1}{r}\right)\tilde{\rho}\right] = 0 \quad (6)$$

where the reduced properties are defined as $\tilde{P} = P/P^*$, $\tilde{T} = T/T^*$, $\tilde{\rho} = v^*/v$, and r is a chain length given by

$$r = MP^*/kT^*\rho^* = M/\rho^* v^* \quad (7)$$

P^*, T^*, ρ^*, v^*, and M are the characteristic pressure, temperature, density, hard core volume per mer, and weight-average molecular weight, respectively. Mixing rules for the characteristic parameters used here are the ones given by Sanchez and Lacombe.[19]

In this theory, a bare interaction energy density, ΔP^*, replaces the B in the Flory–Huggins theory. The net interaction energies for copolymer–copolymer blends can be expanded, via the binary interaction model, in terms of monomer unit pair interactions, ΔP_{ij}^*, in analogy with eq. (4):

$$\Delta P^* = \Delta P_{13}^*\phi_1' + \Delta P_{23}^*\phi_2' - \Delta P_{12}^*\phi_1'\phi_2' \quad (8)$$

and in analogy with eq. (5):

$$\Delta P^* = \Delta P_{12}^*\phi_2'(\phi_2' - \phi_3'') + \Delta P_{13}^*\phi_3''(\phi_3'' - \phi_2') + \Delta P_{23}^*\phi_2'\phi_3'' \quad (9)$$

where ϕ_k' and ϕ_k'' refer to hard-core volume fractions. The spinodal condition for a binary mixture is given by

$$\frac{d^2G}{d\phi_1^2} = \frac{1}{2}\left[\frac{1}{r_1\phi_1} + \frac{1}{r_2\phi_2}\right] - \tilde{\rho}\left[\Delta P^* v^*/kT + \frac{1}{2}\psi^2\tilde{T}P^*\beta\right] = 0 \quad (10)$$

where ψ is a dimensionless function described elsewhere[19] and β is the isothermal compressibility. The Flory–Huggins interaction energy, defined by eq. (2), can be expressed in terms of the bare in-

Table I SMMA and SMA Copolymers Used in This Study

Polymer	Wt % MMA or MA	Molecular Weight Information[a]	T_g (°C)	Source
SMMA4.5	4.5	$[\eta]$ = 0.32 dl/g	98	Synthesized
SMMA9	9.0	$\bar{M}_n$ = 44,000 $\bar{M}_w$ = 96,000	98	Synthesized
SMMA12.8	12.8	$\bar{M}_n$ = 67,000 $\bar{M}_w$ = 164,000	98	Synthesized
SMMA20.5	20.5	$\bar{M}_n$ = 120,000 $\bar{M}_w$ = 270,000	98	Richardson Polymer [NOAN 81]
SMMA38.5	38.5	$\bar{M}_n$ = 67,000 $\bar{M}_w$ = 130,000	103	Synthesized
SMMA45.9	45.9	$\bar{M}_n$ = 91,000 $\bar{M}_w$ = 150,000	104	Synthesized
SMMA50.3	50.3	$\bar{M}_n$ = 98,000 $\bar{M}_w$ = 200,000	102	Synthesized
SMMA58.5	58.5	$\bar{M}_n$ = 120,000 $\bar{M}_w$ = 240,000	105	Richardson Polymer [RPC100]
SMMA69.3	69.3	$\bar{M}_n$ = 81,000 $\bar{M}_w$ = 180,000	105	Synthesized
SMMA85.1	85.1	$\bar{M}_n$ = 100,000 $\bar{M}_w$ = 200,000	108	Synthesized
SMA2	2.0	$\bar{M}_n$ = 183,000 $\bar{M}_w$ = 319,500	104	Arco Chemical Co.
SMA4.7	4.7	$\bar{M}_n$ = 94,000 $\bar{M}_w$ = 179,000	104	Dow Chemical Co.
SMA6	6.0	$\bar{M}_n$ = 152,000 $\bar{M}_w$ = 273,000	113	Arco Chemical Co.
SMA8	8.0	$\bar{M}_n$ = 100,000 $\bar{M}_w$ = 200,000	116	Arco Chemical Co. (Dylark 232)
SMA10[b]	10.7	$\bar{M}_n$ = 100,000 $\bar{M}_w$ = 210,000	120	Arco Chemical Co. (Dylark 238)
SMA12[c]	12.2	$\bar{M}_n$ = 90,500 $\bar{M}_w$ = 190,000	123	Arco Chemical Co. (Dylark 480)
SMA14	14.0	$\bar{M}_n$ = 90,000 $\bar{M}_w$ = 180,000	126	Arco Chemical Co. (Dylark 332)
SMA18	18.1	$\bar{M}_n$ = 91,500 $\bar{M}_w$ = 260,000	137	Dow Chemical Co.
SMA25	25.0	$\bar{M}_n$ = 69,700 $\bar{M}_w$ = 252,000	149	Monsanto Co.
SMA33			155	Dow Chemical Co.
SMA48	48.5	$\bar{M}_n$ = 50,000 $\bar{M}_w$ = 278,000	178	Scientific Polymer Products

[a] From GPC analysis using polystyrene standards.
[b] 5 wt % rubber particles were removed by a centrifugal separater using methyl ethyl ketone as the solvent.
[c] 16 wt % rubber particles were removed by a centrifugal separater using methyl ethyl ketone as the solvent.

teraction energy in the Sanchez–Lacombe theory, as shown previously,[1,24] by the relation

$$B_{sc} = \tilde{\rho}\Delta P^* + \left\{[P_2^* - P_1^* + (\phi_2 - \phi_1)\Delta P^*] + \frac{RT}{\tilde{\rho}}\left(\frac{1}{r_1^0 v_1^*} - \frac{1}{r_2^0 v_2^*}\right) + -RT\left(\frac{\ln(1-\tilde{\rho})}{\tilde{\rho}^2} + \frac{1}{\tilde{\rho}}\right)\left(\frac{1}{v_1^*} - \frac{1}{v_2^*}\right)\right\}^2 \Bigg/ \left\{\frac{2RT}{v^*}\left[\frac{2\ln(1-\tilde{\rho})}{\tilde{\rho}^3} + \frac{1}{\tilde{\rho}^2(1-\tilde{\rho})} + \frac{(1-1/r)}{\tilde{\rho}^2}\right]\right\} \quad (11)$$

MATERIALS AND PROCEDURES

The chemical composition, molecular weights, and T_g information for the polymers used in this study are given in Tables I and II. The SMA copolymers were obtained from other sources, whereas the SMMA copolymers were mostly synthesized in this laboratory via radical polymerization using azobisisobutyronitrile (AIBN) at 75°C. Methyl acrylate (2–4 wt % of the monomer mixture) was added to prevent unzipping at elevated temperatures. Copolymer compositions were determined by ^{1}H-NMR, on a acrylate-free basis. Molecular weight information for the copolymers were obtained using gel permeation chromatography based on polystyrene standards.

Table II Other Polymers Used in This Study

Polymer	Molecular Weight Information	Description	Source
SAN3.5	$\bar{M}_n$ = 93,000 $\bar{M}_w$ = 204,000	3.5% AN	Asahi
SAN6.3	$\bar{M}_n$ = 121,000 $\bar{M}_w$ = 343,000	6.3% AN	Dow Chemical Co.
SAN9.5	$\bar{M}_n$ = 94,700 $\bar{M}_w$ = 196,000	9.5% AN	Asahi
SAN13.5	—	13.5% AN	Ashai
SAN14.7	$\bar{M}_n$ = 83,000 $\bar{M}_w$ = 182,000	14.7% AN	Asahi
SAN15.5	—	15.5% AN	Asahi
SAN19.5	$\bar{M}_n$ = 84,300 $\bar{M}_w$ = 179,000	19.5% AN	Asahi
SAN25	$\bar{M}_n$ = 77,000 $\bar{M}_w$ = 152,000	25% AN	Asahi
SAN28	—	28% AN	Asahi
SAN30	$\bar{M}_n$ = 81,000 $\bar{M}_w$ = 168,000	30% AN	Dow Chemical Co.
SAN33	$\bar{M}_n$ = 68,000 $\bar{M}_w$ = 146,000	33% AN	Monsanto Co.
SAN34	$\bar{M}_n$ = 73,000 $\bar{M}_w$ = 145,000	34% AN	Asahi
SAN40	$\bar{M}_n$ = 61,000 $\bar{M}_w$ = 122,000	40% AN	Ashai
PMMA	$\bar{M}_n$ = 52,900 $\bar{M}_w$ = 105,400	—	Rohm & Hass V(811)100
TMPC	$\bar{M}_w$ = 33,000	—	Bayer AG
PPO	$\bar{M}_n$ = 29,400 $\bar{M}_w$ = 39,000	—	General Electric Co.

Blend films were prepared mainly by hot casting from different solvents into a Petri dish heated to 60°C. The cast films were dried at 60°C for 10 min in a circulating oven until most of the solvent evaporated before further drying in a vacuum oven at 170°C, unless mentioned otherwise. Most of the phase-separation temperatures reported here reflect an equilibrium phase diagram of the LCST type.[1,24,26]

The T_g of the blends were measured using a Perkin-Elmer DSC-7 at a scanning rate of 20°C/min. The onset of the change in heat capacity is defined as the T_g. Phase-separation temperatures, i.e., LCST behavior, were estimated by isothermal annealing in the DSC sample holder at various temperatures for 4–5 min, after which the sample was quickly quenched to room temperature before running the DSC scan, as described in previous articles.[24–27] Phase-separation temperatures were also estimated by observing where films first turn cloudy during annealing blend samples on a hot stage (Mettler, FP82 HT) equipped with a temperature controller (Mettler, FP80 HT).

The density of the SMA copolymers were determined at 30°C by a density gradient column using calcium nitrate solutions. The pressure–volume–temperature (PVT) properties for the SMA copolymers were obtained using the Gnomix PVT apparatus by measuring the changes in specific volume as a function of pressure and temperature. The sample was compressed along 31 isotherms from 30 to 270°C, spaced about 15–20°C apart, with volume data recorded from 10 to 200 MPa at pressure intervals of 10 MPa.

RESULTS AND DISCUSSION

Blends of SMA Copolymers with SMMA Copolymers

Figure 1 shows the miscibility map for 50/50 wt % blends of SMA copolymers with SMMA copolymers with the miscible and immiscible blends, as prepared, indicated by open and closed points, respectively. As expected, blend films prepared by solution casting from tetrahydrofuran (THF) were transparent for miscible blends and cloudy for immiscible blends. Since the T_g and refractive indices for SMA and SMMA copolymers with low comonomer contents are very close, difficulty arises in distinguishing whether their blends are miscible or not, as indicated by the symbol (+) in Figure 1. The numbers beside the open points refer to the phase-separation temperatures observed. Thus, Figure 1 is more than a simple isothermal phase map at the drying temperature of 170°C. Miscible blends that appeared to have phase-separation temperatures lower than 170°C were dried at temperatures about 20°C above the T_g. Those with phase-separation temperatures above 170°C were tested for phase reversibility to reflect the equilibrium phase diagram by annealing the samples 20°C below the phase-separation temperatures for 1 day. After this treatment, the samples were transparent and DSC thermograms showed a single T_g behavior. Blends with cloud points lower than 170°C did not become homogeneous after the same thermal treatment, possibly because of kinetic factors. As a consequence, the phase-separation temperatures below 170°C must be regarded as somewhat tentative. Note that for a fixed MA content in the SMA copolymer the phase-separation temperatures generally increase as the MMA content in the SMMA copolymer increases. On the other hand, the phase-separation temperatures tend to decrease as the MA content in the SMA copolymer increases for fixed MMA content of the SMMA copolymer. Figure 2 illustrates the T_g behavior of blends of SMA14 with selected SMMA copolymers.

The miscible region shown in Figure 1 encompasses the previously reported miscibility window for blends of PMMA with SMA copolymers. Brannock et al.[29] found that these blends exhibited miscibility for MA contents ranging from 8 to 33 wt % MA. These homogeneous blends were obtained by melt mixing of the polymers. Cloud points were also observed for some of these miscible blends. Figure 1 shows that PMMA blends with SMA copolymers, prepared using the hot-casting method described previously, are miscible from 10 to 33 wt % MA in SMA copolymers; the blend of PMMA with SMA8 was judged immiscible in this work. The discrepancy in the miscibility region reported here compared to that reported by Brannock et al. is most likely related to some difficult issues of achieving equilibrium mixing discussed previously.[29] The phase-separation temperatures for all of the miscible blends of PMMA with SMA copolymers prepared here were judged to be above the thermal degradation limit, which differs somewhat from the results reported by Brannock et al.[29] In any case, the phase-separation temperatures reported are only approximate values.

An approximate set of Flory–Huggins interaction energies, B_{ij}, can be obtained by fitting eqs. (4) and (5) to the experimental copolymer–copolymer composition miscibility map shown in Figure 1 using a computer program[1,20] that minimizes an objective function defined as the sum of the square of the orthogonal distances of the experimental data points to the theoretical boundary curve. As mentioned earlier, for copolymer–copolymer blends containing

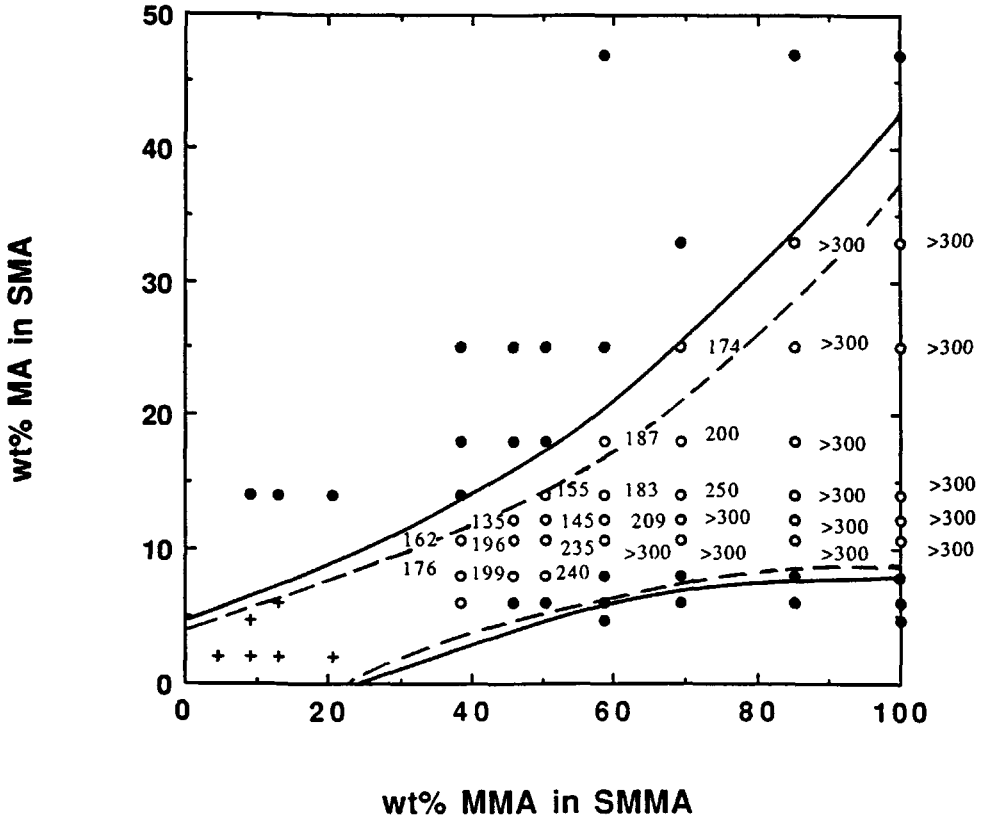

Figure 1 Miscibility map for 50/50 wt % blends of SMA copolymers with SMMA copolymers: (○) miscible; (●) immiscible; (+) T_g and refractive indices of the two copolymers are too close to judge whether these blends were miscible or immiscible. The numbers beside the open points refer to phase-separation temperatures observed for the miscible blends. The solid lines were calculated with $B_{S/MMA}$ = 0.22, $B_{MMA/MA}$ = 7.18, and $B_{S/MA}$ = 10.7 cal/cm^3, whereas the dashed lines were calculated with $B_{S/MMA}$ = 0.22, $B_{MMA/MA}$ = 10.6, and $B_{S/MA}$ = 15 cal/cm^3 using eqs. (6) and (7) and $\bar{M}_w$ = 200,000 for SMMA copolymers and $\bar{M}_w$ = 180,000 for SMA copolymers.

a common monomer, all the absolute B_{ij} values can, in principle, be extracted without prior knowledge of any B_{ij} values.[28] The set of interaction energies found by this procedure is $B_{S/MMA}$ = 0.22, $B_{MMA/MA}$ = 7.18, and $B_{S/MA}$ = 10.7 cal/cm^3. This set of B_{ij} values reproduces the experimental miscibility region fairly well, as seen by the solid line in Figure 1. Note that the value of $B_{S/MMA}$ deduced here corresponds well to previous estimates from other blend systems.[1,22,24,30] Kim et al.[31] reported a value of 7.32 cal/cm^3 for the S/MA pair, obtained from heat of mixing measurements using appropriate liquid analogs. On the other hand, Brannock et al.[29] found that $B_{S/MA}$ = 14.9 and $B_{MMA/MA}$ = 9.30 cal/cm^3 from the miscibility boundaries of blends of PMMA with SMA copolymers. The set of B_{ij} values estimated here predicts negative net interaction energies (as low as −0.01 to −0.11 cal/cm^3) within the region encompassed by the two solid lines. Because of this, blends within this region are predicted to be miscible regardless of the molecular weight of the components.

Brannock et al.[29] reported a much higher value for $B_{S/MA}$ (i.e., 14.9 cal/cm^3) than found by the fitting procedure described above. It is instructive to explore the sensitivity of these boundaries to the B_{ij} values. As an alternative, we set $B_{S/MMA}$ = 0.22 and $B_{S/MA}$ = 15 cal/cm^3. Assuming that SMA9 represents the edge of the miscibility boundary with PMMA leads to $B_{MMA/MA}$ = 10.6 cal/cm^3. The dashed lines in Figure 1 show the miscibility region predicted by this set of interaction energies. Note that this miscibility region is smaller than that predicted above. The upper boundary is shifted downward significantly; however, there is little change in the lower boundary line. For this set of interaction

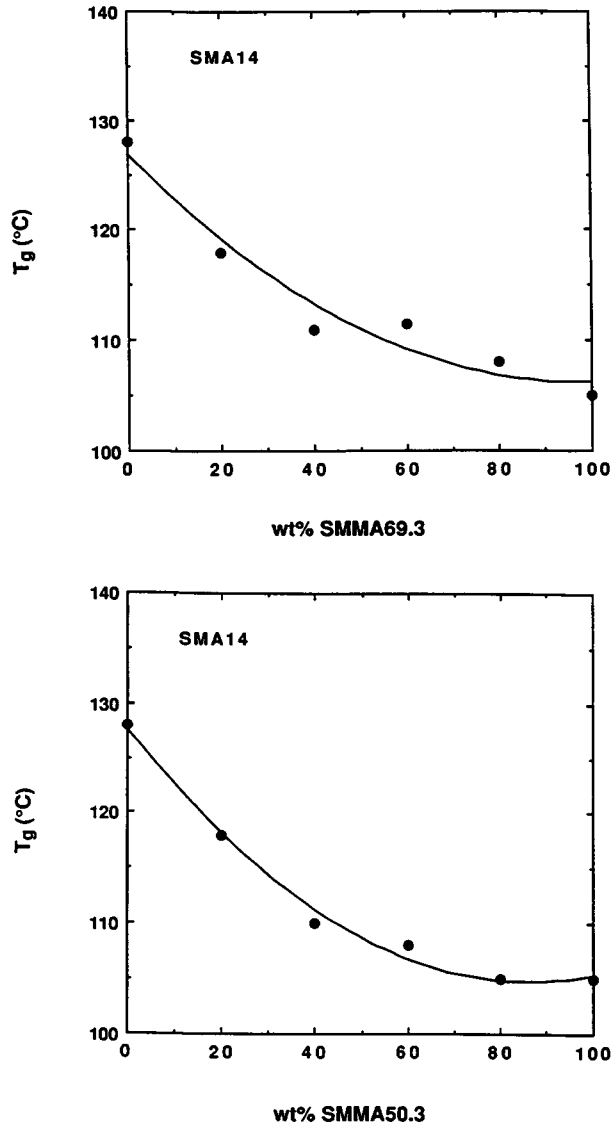

Figure 2 Glass transition temperatures (onset method) for SMA14 blends with selected SMMA copolymers.

energies, there are three blends (MA content 18 wt % and higher) declared miscible by experiment that are not included in the predicted miscible zone. However, the slight shift in the lower limit of MA content gives better agreement with the experiment. Both sets of interaction energies describe the miscibility region fairly well, and with the data available, we cannot come to a conclusion as to which set of interaction energies is more nearly correct.

The B_{ij} values at 170°C can be used to calculate the Sanchez–Lacombe interaction energies, ΔP^*_{ij}, using eq. (11) once the characteristic parameters for the copolymers are known. The characteristic parameters for SMMA copolymers were calculated from results described previously.[25] However, those for SMA copolymers had to be determined. Figure 3 shows the experimental PVT data for SMA14, measured for this purpose. The bold line refers to the pressure dependence of T_g, defined as the intersection of the isobars above and below the transition region. Complete PVT data for the other SMA copolymers are given elsewhere[20] along with the parameters of the empirical Tait equation fitted to the experimental data for both the melt and glassy states.

Characteristic parameters for the SMA copolymers were determined by a nonlinear least-squares fit of the experimental PVT data to the Sanchez–Lacombe equation of state.[17–19] Because the form of the theoretical equation of state cannot precisely describe the experimental PVT data, as explained elsewhere,[20,25] somewhat different characteristic parameters are obtained depending on the temperature range over which the data are fitted. The parameters deduced for two separate temperature ranges are shown in Table III. The phase-separation temperatures in Figure 1 fall primarily within the 150–200°C range, so for consistency, these values were used to evaluate the interaction energies from the experimental observations. Figure 4 shows how the characteristic parameters for the temperature range of 150–200°C change with the MA content of the SMA copolymers. Prior work with other copolymers[25] has shown that the effect of comonomer content on the characteristic parameters is well described by the mixing rules mentioned earlier.[25] The closed points in Figure 4 represent the characteristic parameters determined by a nonlinear least-squares fit of the experimental PVT data to eq. (6), whereas the lines correspond to the best fit of these points to the mixing rules. As seen in Figure 4(c), ρ^* follows a well-defined trend; however, more scatter is noted in the T^* and P^* plots. The level of uncertainties that exists for the latter have been shown to be rather unimportant for present purposes.[20] In the following interaction energy calculations, the T^* values for SMA copolymers obtained via fitting of the copolymer characteristic parameters to the mixing rules will be used.

The Sanchez–Lacombe ΔP^*_{ij} deduced from the original set of B_{ij} values at 170°C using eq. (11) and characteristic parameters for SMA and SMMA copolymers are as follows: $\Delta P^*_{S/MMA} = 0.23$, $\Delta P^*_{MMA/MA} = 7.28$, and $\Delta P^*_{S/MA} = 10.9$ cal/cm^3. Bare interaction energies, ΔP^*, calculated from the ΔP^*_{ij} values above are all negative and showed the same trend as that observed for net interaction energies calculated using the B_{ij} values deduced pre-

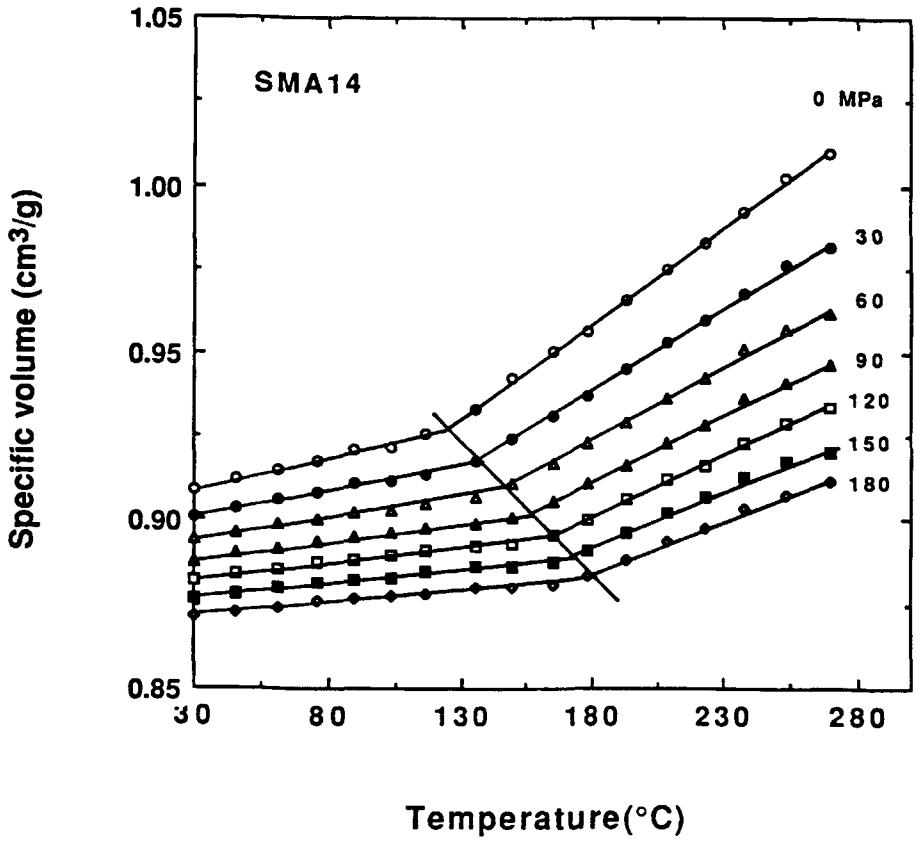

Figure 3 Specific volume of SMA14 as a function of temperature and pressure.

viously. However, the ΔP^* calculated from these ΔP^*_{ij} predict phase-separation temperatures that are about 200°C higher than that observed. This no doubt reflects some inaccuracy in the B_{ij} values on which the estimates of ΔP^*_{ij} are based. The predicted phase-separation temperatures are extremely sensitive to the values of ΔP^* used in the calculation; an increase in the ΔP^* by only 0.02 cal/cm^3 would lower the phase-separation temperatures by 200°C.

The ΔP^*_{ij} values evaluated from the alternate B_{ij} set mentioned above (i.e., $B_{S/MMA} = 0.22$, $B_{MMA/MA} = 10.6$, and $B_{S/MA} = 15$ cal/cm^3) are $\Delta P^*_{S/MMA} = 0.23$, $\Delta P^*_{MMA/MA} = 10.9$, and $\Delta P^*_{S/MA} = 15.5$ cal/cm^3. The ΔP^* values deduced using this ΔP^*_{ij} set are more negative within the miscible region than are those determined from the former ΔP^*_{ij} set. These ΔP^* predict phase-separation temperatures about 350°C higher than those observed experimentally. Since

Table III Sanchez–Lacombe Equation-of-state Parameters for PS and SMA Copolymers

	Temperature Range 150–200°C			Temperature Range 220–270°C		
Polymer	ρ^* (g/cm^3)	P^* (bar)	T^* (K)	ρ^* (g/cm^3)	P^* (bar)	T^* (K)
PS	1.109	3970	751	1.092	3730	810
SMA2	1.119	4180	735	1.095	3900	793
SMA8	1.150	4250	741	1.137	4220	796
SMA14	1.171	4220	754	1.146	3880	818
SMA18	1.186	4560	757	1.155	3860	830
SMA25	1.213	4370	786	1.221	5150	775

Characteristic parameters obtained over the range of 0–50 MPa.

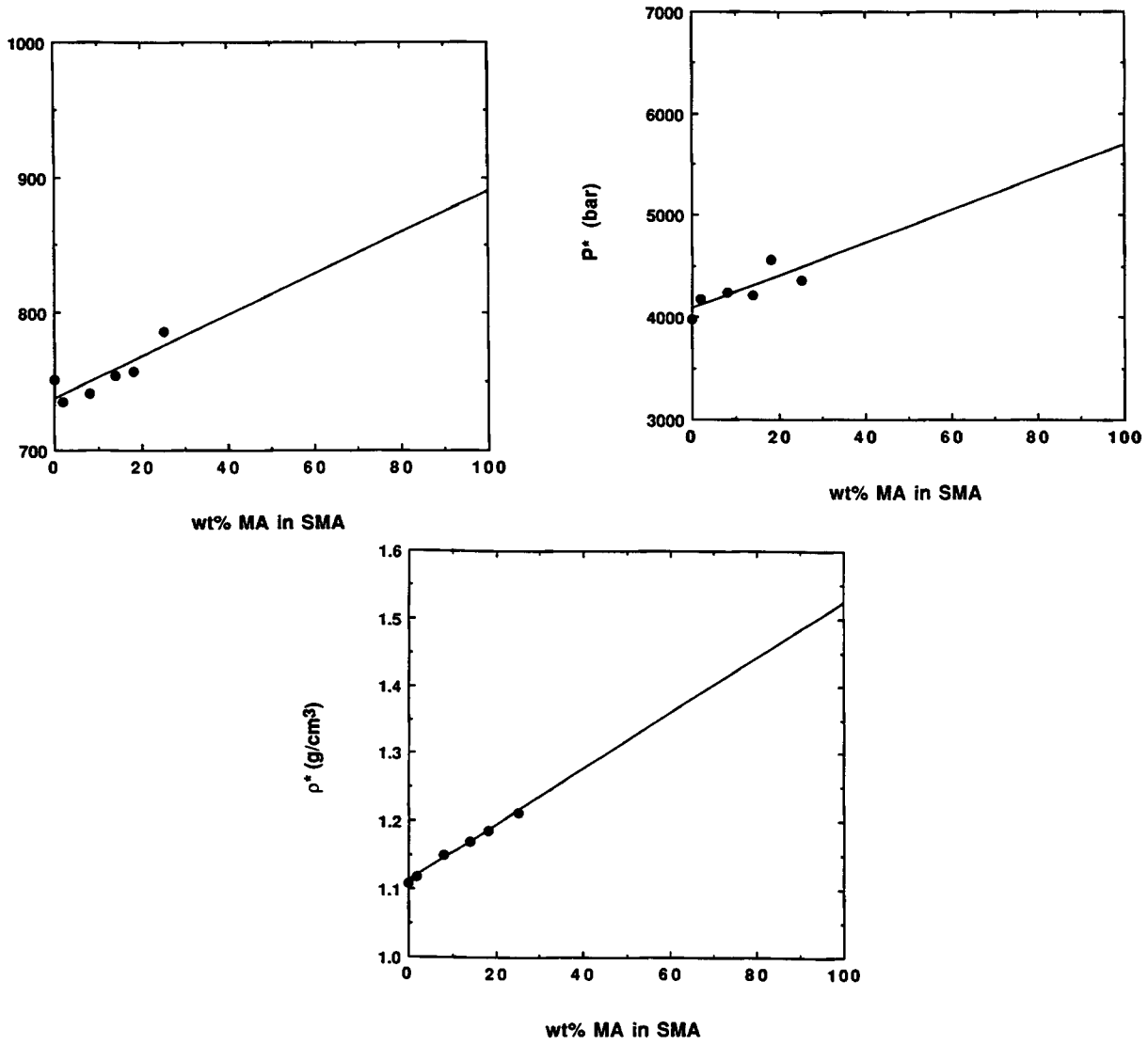

Figure 4 Lattice fluid characteristic parameters for SMA copolymers for the temperature range of 150–200°C: (a) characteristic temperature; (b) characteristic pressure; (c) characteristic density. Lines show the best fit of experimental characteristic parameters to the mixing rule equations.

the information on phase-separation temperatures for this system is so sparse and limited in accuracy, a more refined estimate of ΔP_{ij}^{*} values from phase diagram information is not justified.

Blends of SMA Copolymers with SAN Copolymers

Blends of SMA copolymers with SAN copolymers have been examined by several authors.[31–35] The miscibility region of the blends prepared by Kressler et al.[34] and Aoki[35] were analyzed by differential scanning calorimetry and dynamic mechanical testing, respectively. Kim et al.[31] reported that miscibility is aided by a weak exothermic interaction between the MA and AN units. The value of the pair interaction energies in this blend system were obtained by measuring the heats of mixing for appropriate liquid analogs of the monomer units using both the Flory–Huggins theory and the Sanchez–Lacombe theory. In this study, the miscible/immiscible boundaries were redetermined and attempts were made to determine phase-separation temperatures for all miscible blends. A consistent set of binary interaction energies should describe the observed miscibility boundaries in the copolymer–copolymer composition map and give the correct

phase diagram for each blend. Figure 5 shows the miscibility region for blends of SMA with SAN copolymers observed in this study. The miscible and immiscible blends, prepared by hot casting from THF, were judged by T_g and blend film clarity. Blends of the two copolymers are miscible when their MA and AN comonomer contents are not too different, indicating that there is an exothermic interaction between the MA and AN monomer units.[31] Table IV shows the phase-separation temperatures obtained for the miscible blends. However, most of these blends did not phase-separate on heating prior to thermal decomposition.

Since there were few miscible blends that show phase-separation temperatures, the Flory–Huggins binary interaction energies were obtained by mapping the copolymer–copolymer composition miscibility boundaries. As mentioned previously, the absolute B_{ij} values can be obtained, in principle, without prior knowledge of any one of these values for blends of copolymer–copolymer systems containing a common monomer. Using the computer program previously mentioned,[1,20] the set of B_{ij} values that best separate the miscible and immiscible regions were found to be $B_{S/AN} = 6.8$, $B_{MA/AN} = -0.31$, and $B_{S/MA} = 10.6$ cal/cm^3. The current B_{ij} values agree rather well with those from other sources. For example, the $B_{AN/MA}$ is weakly attractive, which corresponds well to $B_{MA/AN} = -0.34$ cal/cm^3 from heats of mixing of liquid analogs[31] and -0.38 cal/cm^3 from a previous analysis of the miscibility boundaries for blends of SMA with SAN copolymers.[29] However, positive interaction energies were reported for the MA/AN pair by Kressler et al.[34] and Aoki[35] based on studies of SMA/SAN blends. The $B_{S/AN}$ obtained here matches quite well the value of 7.02 cal/cm^3 determined from analysis of the phase behavior of blends of TMPC with SAN copolymers.[25] The $B_{S/MA}$ deduced here matches the value of 10.7 cal/cm^3 estimated from blends of SMA with SMMA copolymers. On the other hand, Brannock et al.[29] and Aoki[35] reported higher values for the S/MA pair interaction. The solid lines in Figure 5 were computed from the set of B_{ij} values above. Note that the calculated lines separate the miscible and immiscible blends quite well. Net interaction energies calculated were mostly negative except for some points near the edge of the miscibility window. As seen in Figure 5, there are some immiscible blends that fall in the predicted miscibility region. For these cases, the proposed set of B_{ij} values do predict immiscibility when the actual weight-average molecular weights of the components are taken into consideration.

As mentioned previously, a value of $B_{S/MA}$ approaching 15 cal/cm^3 has been reported and it is

Table IV Phase-separation Temperatures for the Miscible Blends of 50/50 Wt % SMA with SAN Copolymers

Wt % MA in SMA	Wt % AN in SAN	Phase Separation Temperature (°C)
14	9.5	> 300
	11.5	285
	13.5	250
	15.5	240
18	13.5	> 300
	15.5	> 300
	19.5	> 300
	25	250
25	19.5	> 300
	25	> 300
	33	260
	34	270
47	40	> 300
48.5	40	> 300

Miscible blends of SAN copolymers with SMA copolymers containing less than 14 wt % MA did not phase-separate upon heating prior to thermal degradation.

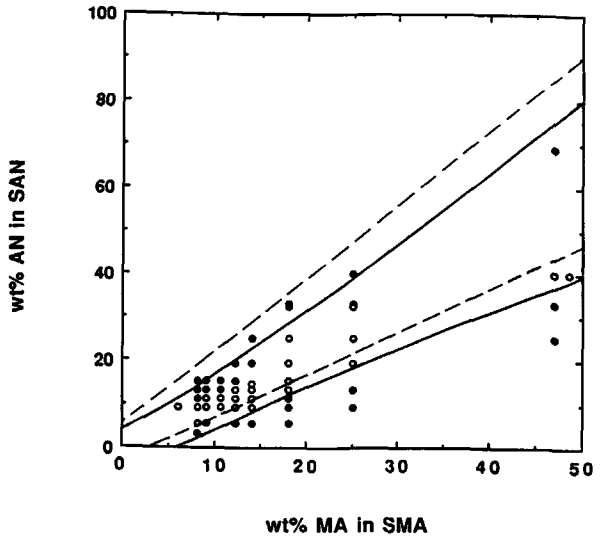

Figure 5 Miscibility map at 170°C for 50/50 wt % blends of SMA copolymers with SAN copolymers: (○) miscible; (●) immiscible. The solid lines were calculated with $B_{S/AN} = 6.8$, $B_{MA/AN} = -0.31$, and $B_{S/MA} = 10.7$ cal/cm^3, whereas the dashed lines were calculated with $B_{S/AN} = 6.8$, $B_{MA/AN} = 0.29$, and $B_{S/MA} = 15$ cal/cm^3 using eqs. (6) and (7) and $\bar{M}_w = 180{,}000$ for SMA copolymers and $\bar{M}_w = 150{,}000$ for SAN copolymers.

interesting to see whether this value is consistent with the experimental observations reported here. For this exercise, we will retain $B_{S/AN} = 6.8$ cal/cm^3 since this value has been repeatedly found or confirmed in previous studies.[1,24,25] The resulting best fit with these values fixed obtained by the computer program previously mentioned[1,20] gives $B_{MA/AN} = 0.29$ cal/cm^3. This positive interaction is in contrast to the negative value obtained from heat of mixing measurements[31] and from analysis of copolymer composition boundaries for blends of SMA with SAN copolymers.[29] In addition, the predicted miscibility region (see dashed lines in Fig. 5) does not match the experimentally observed region very well. Some blends declared immiscible experimentally fall in the predicted miscible zone and vice versa. Retaining $B_{S/AN} = 6.8$ and $B_{S/MA} = 15$ cal/cm^3, a negative interaction of $B_{MA/AN} = -0.1$ or -0.31 cal/cm^3 would shift the upper boundary line higher than the dashed line in Figure 5 and the lower boundary line would lie in between the lower dashed and solid lines in Figure 5. Again, the predicted miscibility region using these interaction energy values would not match the experimentally observed region very well. It appears that the set of interaction energies with $B_{S/MA} = 10.6$ cal/cm^3 gives a better representation of the miscibility region for this blend system.

The B_{ij} set with $B_{S/MA} = 10.6$ cal/cm^3 at 170°C were used to calculate, using eq. (11) and the characteristic parameters for SMA copolymers and SAN copolymers,[25] the following: $\Delta P^*_{S/AN} = 7.37$, $\Delta P^*_{MA/AN} = -0.36$, and $\Delta P^*_{S/MA} = 10.9$ cal/cm^3. Bare interaction energies calculated from these ΔP^*_{ij} values are negative for blends bounded by the solid lines in Figure 5. The points in Figure 6 are the observed phase-separation temperatures (part a) and the bare interaction energies (part b) calculated from them for blends of SMA 14 with SAN copolymers of varying AN content. The ΔP^* calculated from the ΔP^*_{ij} values given above [solid line in Fig. 6(b)] are approximately 0.02–0.03 cal/cm^3 lower than those deduced from the experimental phase-separation temperatures. The open points with arrows in Figure 6(b) are for immiscible blends whose phase-separation temperatures must lie below 170°C. Note that the curve separates the miscible and immiscible blends quite well. The spinodal values [solid line in Fig. 6(a)] deduced using this set of ΔP^*_{ij} predicts higher phase-separation temperatures than observed experimentally; however, the spinodal line defines the miscibility boundary fairly well. The predicted phase-separation temperatures are extremely sensitive to the value of ΔP^* used in the calculations,

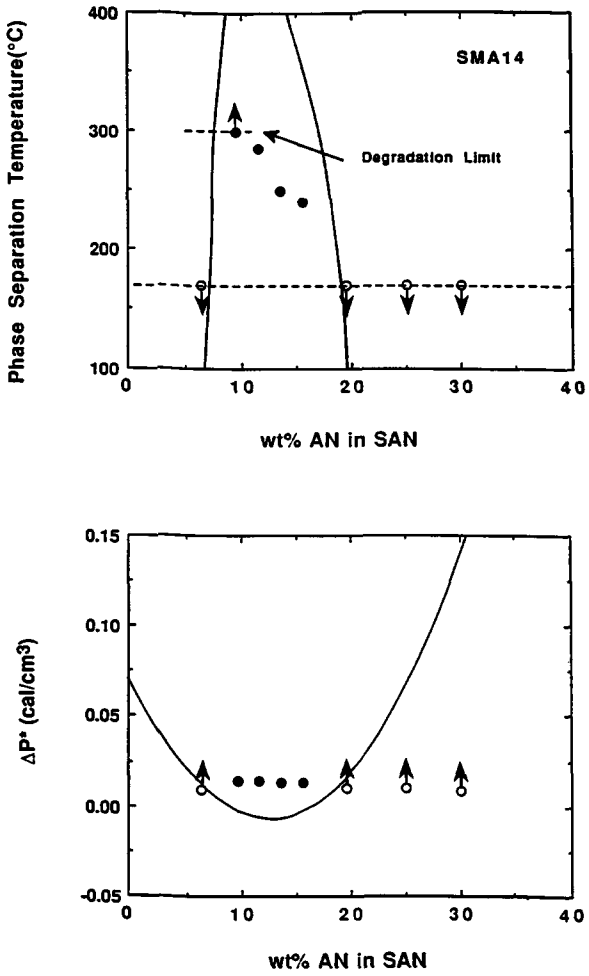

Figure 6 (a) Phase-separation temperatures and (b) bare interaction parameters for 50/50 blends of SMA14 with SAN copolymers. The arrows indicate phase-separation temperatures above the thermal degradation limit. The points in (b) were calculated from the experimental phase diagram using the lattice fluid theory. The solid lines were calculated from $\Delta P^*_{S/AN} = 7.37$, $\Delta P^*_{MA/AN} = -0.36$, and $\Delta P^*_{S/MA} = 10.9$ cal/cm^3.

e.g., an increase in ΔP^* by approximately 0.02 cal/cm^3 will lower the phase-separation temperatures by about 200°C and better match what is observed experimentally. Because the observed phase-separation temperatures are so sparse, it is not possible to use this approach to get more refined estimates of the ΔP^*_{ij} values.

Blends of SMA Copolymers with TMPC

Blends of TMPC with polystyrene and its copolymers with MMA and AN are miscible, within certain limits of comonomer contents, and show LCST behavior at elevated temperatures.[26] Binary pair in-

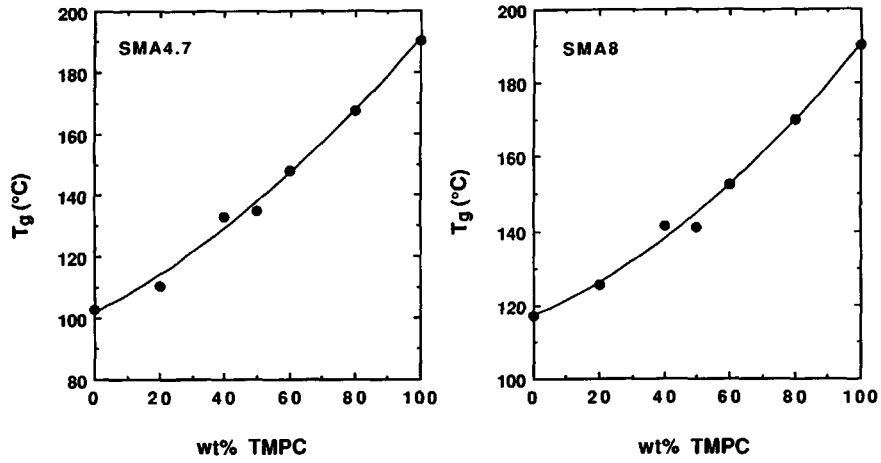

Figure 7 Glass transition temperatures for blends of TMPC with selected SMA copolymers determined by DSC (onset method) at 20°C/min.

teraction energies for each monomer unit pair have been obtained by analysis of various experimental data for these systems using the Sanchez and Lacombe theory.[25]

A similar analysis of blends of TMPC with SMA copolymers is presented here. Blend films of TMPC with SMA copolymers, prepared by hot casting from THF and dried at 180°C, were transparent when the SMA copolymer contained 12 wt % MA or less. These blends showed a single T_g by DSC, as illustrated in Figure 7, for selected SMA copolymers. Blends of TMPC with SMA copolymers with 14 wt % or more MA showed cloudy films and two T_g's were observed by DSC. Phase separation on heating was observed for blends of TMPC with the SMA copolymer containing 2 wt % MA as shown in Figure 8. Miscible blends with SMA copolymers of other MA contents did not phase-separate upon heating prior to thermal decomposition.

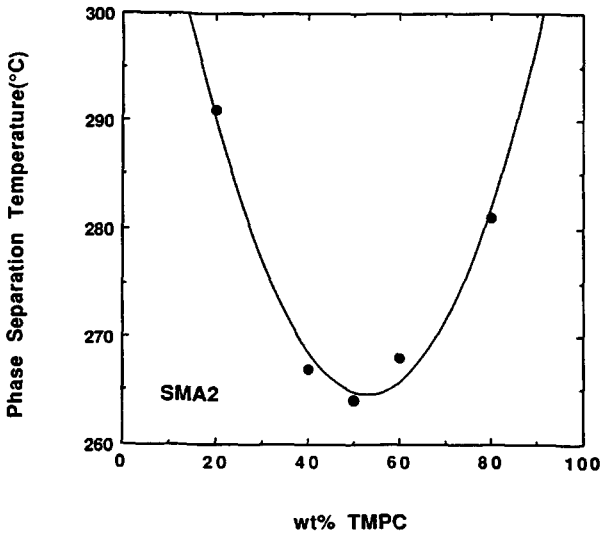

Figure 8 Phase-separation temperatures for blends of TMPC with SMA2.

From the value of $\Delta P^*_{S/TMPC} = -0.17$ cal/cm^3 obtained in a prior analysis of blends of TMPC with polystyrene,[26] we calculated via eq. (11), that $B_{S/TMPC} = -0.14$ cal/cm^3 at 180°C. From the value of $\Delta P^*_{S/MA} = 10.9$ cal/cm^3 obtained from the analysis of blends of SMA copolymers with SMMA copolymers described earlier, we calculated via eq. (11), that $B_{S/MA} = 10.7$ cal/cm^3 at 180°C. Using these values and the observed miscibility limit for blends of SMA copolymers with TMPC at 180°C, we estimated from eq. (3) that $11.3 < B_{TMPC/MA} < 11.7$ cal/cm^3. The corresponding $\Delta P^*_{TMPC/MA}$, from eq. (11), ranges from 11.6 to 11.9 cal/cm^3. We believe that the bare interaction energy for the TMPC/MA pair is closer to 11.9 cal/cm^3 (the corresponding Flory–Huggins parameter $B_{TMPC/MA} = 11.7$ cal/cm^3 at 180°C) since this better matches the experimental phase-separation temperature observed for TMPC blends with SMA2.

Blends of SMA Copolymers with PPO

Blends of PPO and polystyrene are miscible and do not phase-separate on heating prior to decomposition.[24,36–39] Blends of PPO have been reported to be miscible with SAN copolymers containing less than 12.4 wt %.[24,40] Fried and Hanna[41] examined blends of PPO with SMA copolymers containing 8 and 14 wt % MA by DSC and dynamic mechanical analysis. The phase behavior of blends of PPO with other

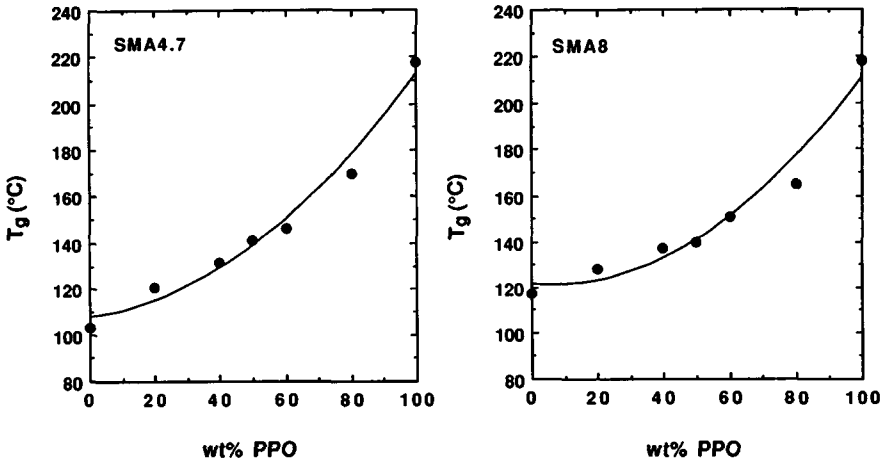

Figure 9 Glass transition temperatures for blends of PPO with selected SMA copolymers determined by DSC (onset method) at 20°C/min.

SMA copolymers was examined more thoroughly here to obtain better estimates of the interaction energies that describe the phase behavior of these blends.

Blends of PPO with SMA copolymers containing 10 wt % MA and less, solution-cast from chloroform, were found to be transparent and exhibited a single T_g. Figure 9 shows the T_g behavior for blends of 50/50 wt % PPO with polystyrene and with selected SMA copolymers. SMA copolymers containing 12 wt % MA or more were found to be immiscible with PPO. None of the miscible blends phase-separated on heating prior to thermal decomposition.

The interaction energy densities were calculated using the same method of analysis for blends of TMPC with SMA copolymers since one miscibility boundary is observed. Gan et al.[24] calculated that $\Delta P^*_{S/PPO} < -0.42$ cal/cm^3 based on the fact that PPO/PS blends do not phase-separate on heating to temperatures of at least 300°C; this corresponds to $B_{S/PPO} < -0.37$ cal/cm^3 at 180°C. From analysis of blends of SMA with SMMA copolymers, $B_{S/MA} = 10.7$ cal/cm^3 at 180°C. From these two values and the miscibility limit for blends of PPO with SMA copolymers, it is estimated that $B_{PPO/MA}$ must lie in the range from 14.2 to 15.1 cal/cm^3. The corresponding $\Delta P^*_{PPO/MA}$ ranges from 14.7 to 15.3 cal/cm^3.

CONCLUSIONS

Miscibility regions for blends of SMA copolymers with styrenic copolymers containing MMA and AN were examined. Some miscible blends of SMA copolymers with SMMA copolymers phase-separate upon heating, whereas others did not prior to thermal degradation. Blends of SMA copolymers with SAN copolymers show miscibility when the MA and AN contents are not too different, as shown by others.[31-35] Most of the miscible blends did not phase-separate before the thermal degradation temperature. Blends of SMA copolymers with TMPC and PPO were also investigated here, and in essentially all cases, the miscible blends did not phase-separate prior to thermal degradation.

Approximate Flory–Huggins interaction energies, B_{ij}, were obtained from mapping the copolymer–copolymer miscibility regions using the binary interaction model for blends of SMA copolymers with SMMA copolymers and with SAN copolymers. Sanchez–Lacombe interaction energies, ΔP^*_{ij}, calculated from the B_{ij} values in these cases, do not predict the phase diagrams very well due to the extreme sensitivity to the ΔP^* values used. For both blend systems, the observed phase-separation temperatures were too sparse to obtain refined estimates using this information. Because of the limited observable LCST behavior for blends of TMPC or PPO with SMA copolymers, it was only possible to obtain upper or lower bounds on certain pair interaction energies for these systems.

Table V lists the interaction energy densities for the various monomer pairs determined from this analysis along with values obtained from other blend systems using various techniques. As shown, the interaction energies determined from this study correspond quite well to previously reported interaction energy values. A negative interaction energy was obtained for the MA/AN pair; however, strong re-

Table V Interaction Parameters (cal/cm^3) for Various Monomer Pairs

	This study		Other Sources					
Interaction Pair	ΔP_{ij}^*	B_{ij} (at T°C)	ΔP_{ij}^*	B_{ij}	χ	System	Method[a]	Refs.
S-MMA	0.23	0.22	0.23			PMMA/SAN	A	24
		(170)		0.30–0.36		PMMA/PS	C	22
			0.15	0.19		TMPC/SMMA	A	25
			0.13			MMA/ChMA copolymers/PS	B	42
				0.18		PMMA/PS/solvent	D	43–45
					0.01	PMMA/SAN	B	46
S-MA	10.9	10.7		14.9		PMMA/SMA	B	29
		(170)			0.18	SMA/SAN	B	34
			7.52	7.32			E	31
				13.0			F	54
MMA-MA	7.28	7.18		9.30		PMMA/SMA	B	29
		(170)			0.2	SMMA/SMA	B	47
S-AN	7.37	6.80	7.37	7.02		TMPC/SAN	A	25
		(170)		6.74		PMMA/SAN	B	48
				8.14		PMMA/SAN	B	49
				8.02		SAN/MMA copolymers with PhMA, ChMA or tBMA	B	20
				6.8		SAN/ChMA/MMA copolymers	B	50
			5.91	3.17			E	31
				4.99		PMMA/SAN	B	51
				8.0		SAN/SAN	B	52
				6.9			E	53
					0.1	SMA/SAN	B	34
				8.41			F	54
MA-AN	−0.36	−0.31		−0.38		SMA/SAN	B	28
		(170)			4×10^{-4}	SMA/SAN	B	34
			−0.36	−0.34			E	31
				0.49			F	54
TMPC-S	−0.17	−0.14	−0.17			TMPC/PS	A	26
		(180)						
TMPC-MA	11.6–11.9	11.3–11.7						
		(170)						
PPO-S	< −0.42	< −0.37	< −0.42			PPO/SAN	B	24
		(180)			−0.1	PPO/PS	B	36
PPO-MA	14.7–15.3	14.2–15.1						
		(180)						

[a] A = Analysis of LCST-type phase diagram. B = Analysis of copolymer miscibility boundaries. C = Critical molecular weight method. D = Light scattering from polymer/polymer/solvent mixtures. E = Heats of mixing of low molecular weight analogs. F = Solubility parameter theory using group contribution methods developed by Hoy.[54]

pulsive interactions were obtained for the MA unit with all other monomer units examined here. The interaction energy values reported here will be useful in the design of multicomponent polymer systems.

Financial support of this work has been provided by the National Science Foundation Grant Nos. DMR-89-00704 and DMR-92-15926 administered by the Division of Material Research—Polymers Program.

REFERENCES

1. P. P. Gan and D. R. Paul, *Polymer,* in press.
2. P. P. Gan and D. R. Paul, *J. Appl. Polym. Sci.,* in press.
3. M. Lu, H. Keskkula, and D. R. Paul, *Polymer,* **34,** 1874 (1993).
4. M. Lu, H. Keskkula, and D. R. Paul, *Polym. Eng. Sci.,* **34,** 33 (1994).

5. V. Triacca, S. Ziaee, J. W. Barlow, H. Keskkula, and D. R. Paul, *Polymer,* **32,** 1401 (1991).
6. T. W. Cheng, H. Keskkula, and D. R. Paul, *Polymer,* **33,** 1606 (1992).
7. N. C. Liu and W. E. Baker, *Adv. Polym. Tech.,* **11,** 249 (1992).
8. R. E. Lavengood and F. M. Silver, *SPE Tech. Pap.,* **33,** 1369 (1987).
9. A. R. Padwa and R. E. Lavengood, Amer. Chem. Soc., *Polymer Preprints,* **33,** 600 (1992).
10. R. Fayt, R. Jerome, and P. Teyssie, *J. Polym. Sci. Polym. Lett. Ed.,* **19,** 79 (1981).
11. R. Fayt, R. Jerome, and P. Teyssie, *J. Polym. Sci. Polym. Phys. Ed.,* **19,** 1269 (1981).
12. R. Fayt, R. Jerome, and P. Teyssie, *J. Polym. Sci. Polym. Phys. Ed.,* **20,** 2209 (1982).
13. R. Fayt, P. Hadjiandreou, R. Jerome, and P. Teyssie, *J. Polym. Sci. Polym. Chem. Ed.,* **23,** 337 (1985).
14. R. Fayt, R. Jerome, and P. Teyssie, *Makromol. Chem.,* **187,** 837 (1986).
15. R. Fayt, R. Jerome, and P. Teyssie, *J. Polym. Sci. Polym. Lett. Ed.,* **24,** 25 (1986).
16. T. Ouhadi, R. Fayt, R. Jerome, and P. Teyssie, *J. Polym. Sci. Polym. Phys. Ed.,* **24,** 973 (1986).
17. I. C. Sanchez and R. H. Lacombe, *J. Phys. Chem.,* **80,** 2352 (1976).
18. I. C. Sanchez and R. H. Lacombe, *J. Polym. Sci. Polym. Lett. Ed.,* **15,** 71 (1977).
19. I. C. Sanchez and R. H. Lacombe, *Macromolecules,* **11,** 1145 (1978).
20. P. P. Gan, PhD Dissertation, The University of Texas at Austin, 1994.
21. T. A. Callaghan, PhD Dissertation, University of Texas at Austin, 1992.
22. T. A. Callaghan and D. R. Paul, *Macromolecules,* **26,** 2439 (1993).
23. T. A. Callaghan and D. R. Paul, *J. Polym. Sci. Part B Polym. Phys.,* **32,** 1813, 1847 (1994).
24. P. P. Gan, D. R. Paul, and A. R. Padwa, *Polymer,* **35,** 1487 (1994).
25. C. K. Kim and D. R. Paul, *Polymer,* **33,** 2089 (1992).
26. C. K. Kim and D. R. Paul, *Polymer,* **33,** 1630 (1992).
27. C. K. Kim, PhD Dissertation, University of Texas at Austin, 1992.
28. C. Zhikuan and F. E. Karasz, *Macromolecules,* **25,** 4716 (1992).
29. G. R. Brannock, J. W. Barlow, and D. R. Paul, *J. Polym. Sci. Part B Polym. Phys.,* **29,** 413 (1991).
30. T. P. Russell, *Macromolecules,* **26,** 5819 (1993).
31. J. H. Kim, J. W. Barlow, and D. R. Paul, *J. Polym. Sci. Polym. Phys. Ed.,* **27,** 223 (1989).
32. W. J. Hall, R. L. Kruse, R. A. Mendelson, and Q. A. Trementozzi, Am. Chem. Soc. Symp. Ser. 229, American Chemical Society, Washington, DC, 1983, p. 49.
33. W. J. Hall, R. L. Kruse, R. A. Mendelson, and Q. A. Trementozzi, *Prep. Am. Chem. Soc. Div. Org. Coat. Plast. Chem.,* **47,** 298 (1982).
34. J. Kressler, H. W. Kammer, G. Schmidt-Naake, and K. Herzog, *Polymer,* **29,** 686 (1988).
35. J. Aoki, *Macromolecules,* **21,** 1277 (1988).
36. R. P. Kambour, J. T. Bendler, and R. C. Bopp, *Macromolecules,* **16,** 753 (1983).
37. A. R. Schultz and B. M. Gendron, *J. Appl. Polym. Sci.,* **16,** 461 (1972).
38. J. Stoelting, F. E. Karasz, and W. J. MacKnight, *Polym. Eng. Sci.,* **10,** 133 (1970).
39. P. S. Tucker and D. R. Paul, *Macromolecules,* **21,** 2801 (1988).
40. J. Kressler and H. W. Kammer, *Acta Polym.,* **11,** 600 (1987).
41. J. R. Fried and G. A. Hanna, *Polym. Eng. Sci.,* **22,** 705 (1982).
42. G. R. Brannock, PhD Dissertation, University of Texas at Austin, 1990.
43. T. Fukuda and H. Inagaki, *Pure Appl. Chem.,* **55,** 1541 (1983).
44. T. Fukuda, M. Nagata, and H. Inagaki, *Macromolecules,* **17,** 548 (1984).
45. T. Fukuda, M. Nagata, and H. Inagaki, *Macromolecules,* **19,** 1411 (1986).
46. M. Suess, J. Kressler, H. W. Kammer, and K. Heinemann, *Polym. Bull.,* **16,** 371 (1986).
47. H. W. Kammer, J. Kressler, B. Kressler, D. Scheller, H. Kroschwitz, and G. Schmidt-Naake, *Acta Polym.,* **40,** 75 (1989).
48. M. Nishimoto, H. Keskkula, and D. R. Paul, *Polymer,* **30,** 1279 (1989).
49. G. R. Brannock, J. W. Barlow, and D. R. Paul, *J. Polym. Sci. Part B Polym. Phys.,* **28,** 871 (1990).
50. M. Nishimoto, H. Keskkula, and D. R. Paul, *Macromolecules,* **23,** 3633 (1990).
51. M. G. Cowie and D. Lath, *Makromol. Chem. Macromol. Symp.,* **16,** 103 (1988).
52. B. J. Schmitt, R. G. Kirste, and J. Jelenic, *J. Makromol. Chem.,* **181,** 1655 (1980).
53. C. H. Lai, PhD Dissertation, University of Texas at Austin, 1988.
54. K. J. Hoy, *J. Paint Technol.,* **42,** 76 (1970).

Received December 20, 1993
Accepted April 12, 1994